



Biomimetic electrospun nanofibrous structures for tissue engineering

Xianfeng Wang^{1,2}, Bin Ding² and Bingyun Li^{1,3,*}

¹Department of Orthopaedics, School of Medicine, West Virginia University, Morgantown, WV 26506, United States

²State Key Laboratory for Modification of Chemical Fibers and Polymer Materials, College of Materials Science and Engineering, Donghua University, Shanghai 201620, China

³WVNano Initiative, Morgantown, WV 26506, United States

Biomimetic nanofibrous scaffolds mimicking important features of the native extracellular matrix provide a promising strategy to restore functions or achieve favorable responses for tissue regeneration. This review provides a brief overview of current state-of-the-art research designing and using biomimetic electrospun nanofibers as scaffolds for tissue engineering. It begins with a brief introduction of electrospinning and nanofibers, with a focus on issues related to the biomimetic design aspects. The review next focuses on several typical biomimetic nanofibrous structures (e.g. aligned, aligned to random, spiral, tubular, and sheath membrane) that have great potential for tissue engineering scaffolds, and describes their fabrication, advantages, and applications in tissue engineering. The review concludes with perspectives on challenges and future directions for design, fabrication, and utilization of scaffolds based on electrospun nanofibers.

Introduction

Tissue engineering is an emerging interdisciplinary field that applies biological and engineering principles to develop biological substitutes that restore, maintain, or improve tissue function [1–4]. It usually requires a scaffold to provide a transitional three-dimensional (3D) support for cell migration, attachment, and proliferation, as well as to provide a vector for delivery of biochemical factors [5,6]. The scaffold should also offer mechanical as well as biological influences to guide the maturation and integration of cells to form tissues [7]. Therefore, the major challenge in tissue engineering is to design and fabricate a suitable scaffold to fulfill the growing needs of the field.

With increasing understanding of the intricate interactions between cells and their microenvironment in tissues, more attention is now focused on the preparation of scaffolds that can imitate the componential and structural aspects of extracellular matrix (ECM) to facilitate cell recruiting/seeding, adhesion, proliferation, differentiation, and neo tissue genesis [3,8,9]. From a structural perspective, natural ECM consists of various interwoven protein

fibers with diameters ranging from tens to hundreds of nanometers [10]. The nanoscale structure of ECM offers a natural network of nanofibers to support cells and to present an instructive background to guide cell behavior [11,12]. Developing scaffolds that imitate the architecture of tissues at the nanoscale is one of the major challenges in the field of tissue engineering [13–15]. The development of nanofibers has greatly improved the scope for preparing scaffolds that can imitate the architecture of natural human tissues at the nanoscale [16].

Various processing techniques (e.g. phase separation, self-assembly, and electrospinning) have been developed to fabricate nanofibrous scaffolds to be used as ECM substitutes (Fig. 1) [9,17–22]. Among them, the electrospinning process has attracted significant attention because of its ability to generate fibers similar to the fibrous structures of native ECM (Fig. 1c) and to process a wide range of materials, as well as the straightforward nature of the process and its cost-effectiveness [23,24]. The large surface area of electrospun nanofibers as well as their porous structure favors cell adhesion, proliferation, migration, and differentiation [25–27]. If necessary, the nanofibers can be further functionalized via incorporation with bioactive species (e.g. enzymes, DNAs, and growth

*Corresponding author: Li, B. (bili@hsc.wvu.edu)

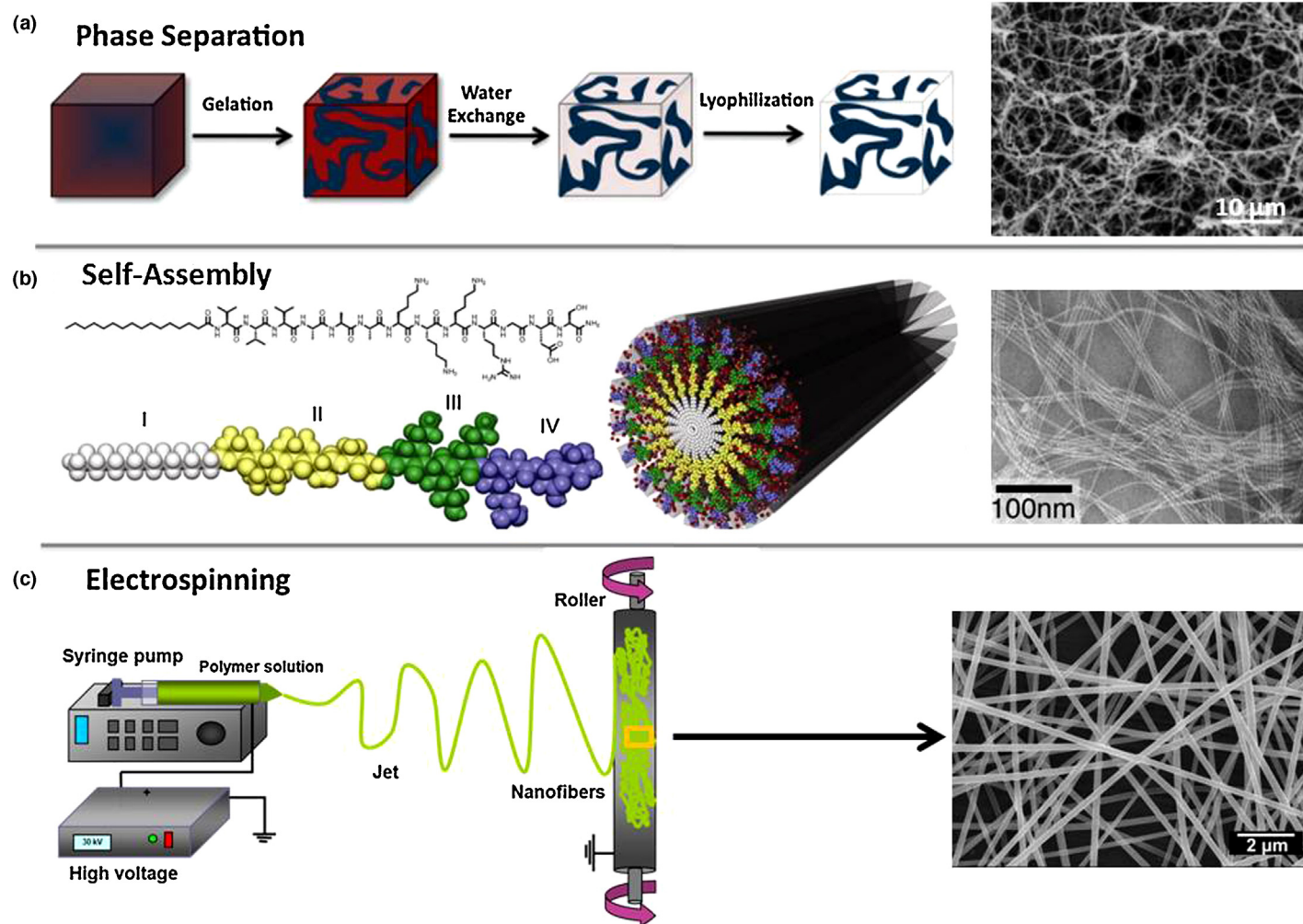


FIGURE 1

Schematic of current techniques (i.e., phase separation, self-assembly, and electrospinning) to create fibrillar structures in synthetic scaffolds. (a) Reprinted with permission from [20]. © 2012 Elsevier B.V. (b) Reprinted with permission from [21]. © 2011 Elsevier B.V. Scanning electron microscopy (SEM) images adapted and reprinted with permission (a) from [17]. © 1999 Wiley-VCH Verlag GmbH & Co. and (b) from [22]. © 2002 The National Academy of Sciences of the USA.

factors) to better control the proliferation and differentiation of cells seeded on the scaffolds [8]. These attributes make electrospun nanofibers well-suited as scaffolds for tissue engineering.

This article gives a brief overview of recent work on designing and using biomimetic electrospun nanofibers as scaffolds for tissue engineering. First, we present a brief introduction to electrospinning and nanofibers, with a focus on issues related to the biomimetic design aspect. We then highlight a variety of biomimetic nanofibrous scaffolds fabricated via electrospinning, describing their fabrication, advantages, and applications in tissue engineering. Finally, we give conclusions along with perspectives on challenges and future directions of biomimetic scaffolds based on electrospun nanofibers.

Electrospinning of nanofibers

Electrospinning (also termed electrostatic spinning) has gained substantial attention in the last two decades triggered mainly by the potential applications of electrospun nanofibers in nanoscience and nanotechnology [28–31]. Particularly, remarkable features such as large specific surface area, high porosity, and

spatial interconnectivity of electrospun nanofibers make them well suited for nutrient transport, cell communication, and efficient cellular responses [32,33]. The standard electrospinning system requires four major components: a spinneret with a metallic needle, a syringe pump, a high-voltage power supply, and a grounded collector (Fig. 1c) [34]. The electric field strength overcomes the surface tension of the droplet and generates a charged liquid jet [35]. The jet is then elongated and whiplashed continuously by electrostatic repulsion until it is deposited on the grounded collector [36]. The solvent evaporates on the way and the jet solidifies to form a nonwoven fibrous membrane. The processing flexibility of this technique enables fiber fabrication from a broad range of precursor materials such as synthetic polymers, natural polymers, semiconductors, ceramics, or their combinations [37,38].

Currently, a variety of natural polymers such as collagen, gelatin, elastin, silk, and synthetic polymers such as poly(L-lactic acid) (PLLA), poly(glycolic acid) (PGA), poly(ϵ -caprolactone) (PCL) and poly(lactic-co-glycolic) acid (PLGA) have been electrospun as biomimetic and temporal substrates to modulate various cellular

activities. However, synthetic or natural polymer alone cannot meet all the requirements for tissue engineering. Synthetic polymers have great flexibility in synthesis and modification, but these polymers lack cell affinity because of their low hydrophilicity and lack of surface cell recognition sites. Compared with synthetic polymers, natural polymers provide good biocompatibility but tend to display poor processing ability and mechanical properties [32]. Therefore, it is desirable to fabricate composite fibrous membranes comprising both synthetic polymers for the backbone and natural polymers for cellular attachment, which might possess not only suitable mechanical properties but also a bioactive surface [39].

Biomimicry via electrospinning

By coordinating the parameters of electrospinning, controllable fibrous structures can be successfully fabricated [40,41] and therefore provide excellent prospects for construction of biomimetic structures. Benefitting from the easily tunable compositions and structures of electrospun fibers, a variety of fascinating structures resembling natural objects (e.g. lotus leaf, silver ragwort leaf, rice leaf, honeycomb, polar bear fur, spider webs, soap-bubble, ECM, etc.) have been successfully biomimicked via electrospinning (Fig. 2) [41,42]. Particularly, biomimetic processing for tissue engineering has focused on emulating or duplicating ECM structures and functions using mostly natural or synthetic components [43]. A detailed review of biomimicry based on the electrospinning technique was recently published by Lin and co-workers [44].

Biomimetic nanofibrous scaffolds for tissue engineering

Nanofibers can be electrospun in various patterns depending on the biomedical application. For example, core-shell fibers can facilitate drug delivery in which drugs will be encapsulated in a nonreactive coating and safely delivered to the target sites [45]. Biomimetic substitutes have been developed to replicate natural tissues for use in the repair of destroyed tissues such as skin, bone, dura mater, sciatic nerve, articular cartilage, and tendon in order to improve functional outcomes (Fig. 3) [8,46,47]. In skin tissue regeneration, for example, nanofibers have shown great potential to mimic skin ECM in both morphology and composition, and thus may be promising tissue engineering scaffolds for skin substitutes [48]. The high surface area of nanofibrous scaffolds allows oxygen permeability and prevents fluid accumulation at the wound site, making them ideal substrates for wound dressings [45]. Therefore, it is important to understand the structural and biological properties of tissues in order to gain insight into choosing the materials that best suit reconstruction of these tissues [33]. Bone tissue, as an example, has a hierarchical organization over length scales ranging from macro- to nano-structured (ECM) components [2]. When designing biomimetic scaffolds for bone tissue engineering, the following aspects should be considered: They must (1) mimic the nanofibrous collagen ECM; (2) be highly porous to allow for cell ingrowth and efficient mass transport of nutrients, oxygen, growth factors, and waste products; and (3) be able to withstand mechanical stresses during tissue neogenesis

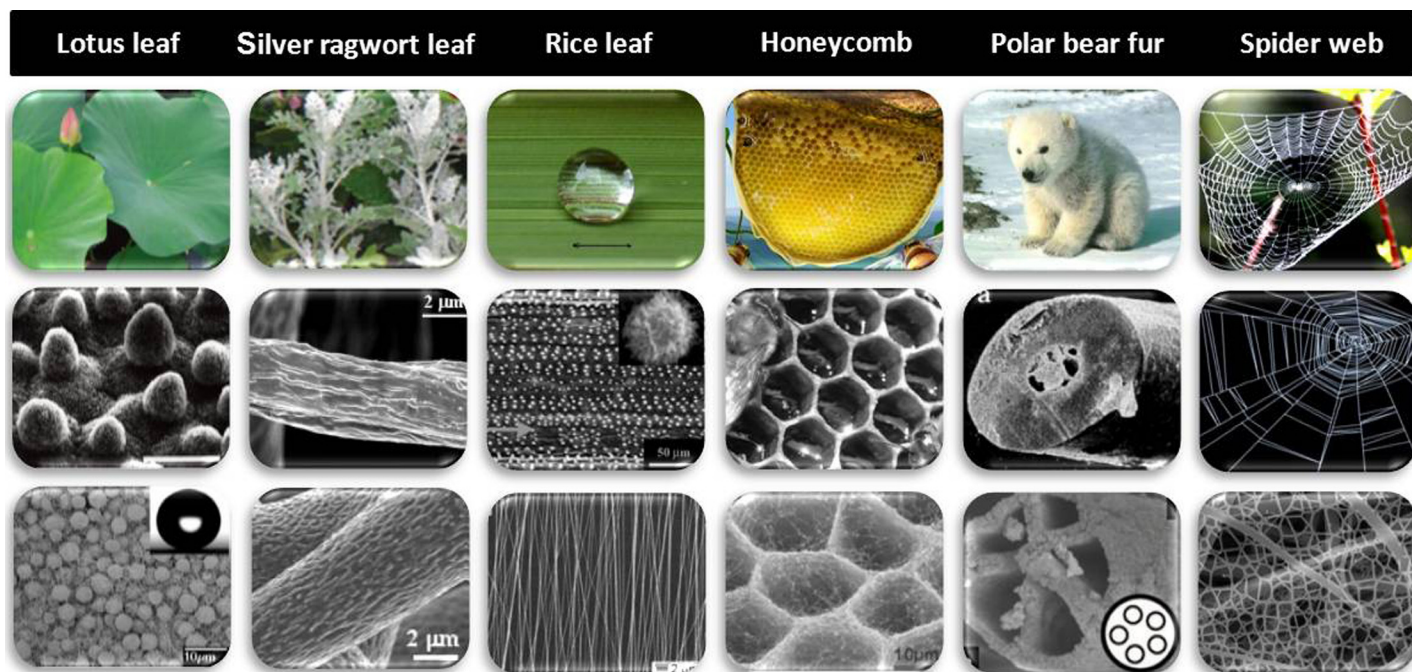


FIGURE 2

Biomimetic electrospun nanofibrous structures inspired from nature. In each case the first row shows a photograph of the biological feature, the second row shows the optical or SEM images of corresponding micro- and nanometer-scale structures, and the third row shows the SEM images of inspired electrospun nanofibrous structures. Lotus leaf: Reprinted with permission from [95]. © 2008 Royal Society of Chemistry; Reprinted with permission from [96]. © 1997 Springer-Verlag; Reprinted with permission from [97]. © 2004 WILEY-VCH Verlag GmbH & Co. Silver ragwort leaf: Reprinted with permission from [44]. © 2012 Taylor & Francis; Reprinted with permission from [98]. © 2006 IOP Publishing Ltd. Rice leaf: Reprinted with permission from [99]. © 2007 Elsevier B.V.; Reprinted with permission from [100]. © 2002 WILEY-VCH Verlag GmbH & Co; Reprinted with permission from [101]. © 2003 American Chemical Society. Honeycomb: Reprinted with permission from Kellix. © 2011 Droid Life: A Droid Community Blog; Reprinted with permission from [102]. © 2011 American Chemical Society. Polar bear: Reprinted with permission from Monnett. © 2011-Salient News; Reprinted with permission from [103]. © 1980 Optical Society of America; Reprinted with permission from [104]. © 2007 American Chemical Society. Spider web: Reprinted with permission from [92]. © 2011 Royal Society of Chemistry.

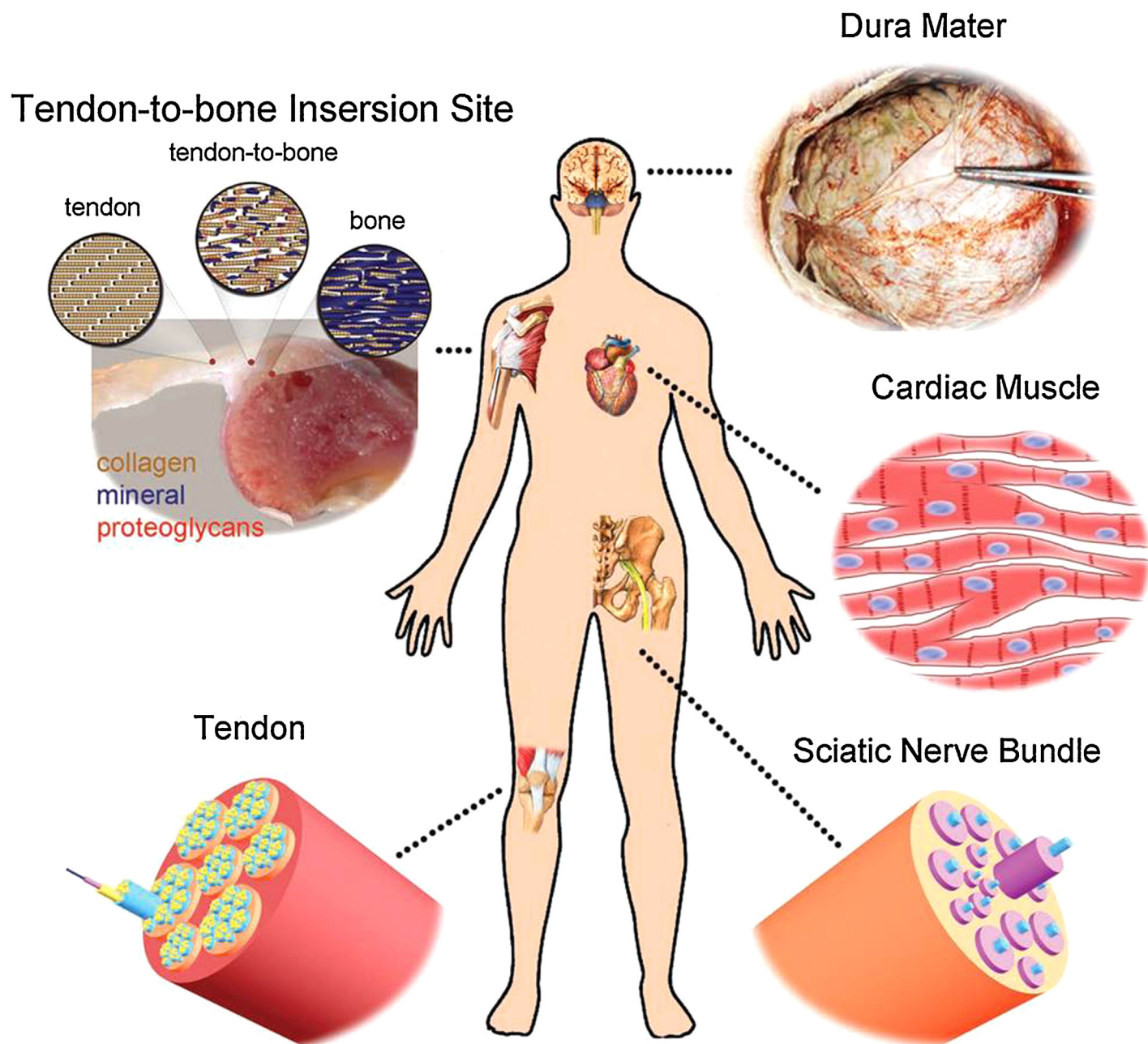


FIGURE 3

Illustration of some typical examples of tissues in the human body whose regeneration would benefit from the use of nanofiber-based scaffolds that could be readily fabricated by electrospinning. Reprinted with permission from [8]. © 2012 Wiley-VCH Verlag GmbH & Co.

[9,49,50]. In this section, we discuss several biomimetic nanofibrous scaffolds (from simple to complex) fabricated via electrospinning and describe their fabrication, advantages, and applications in tissue engineering.

Aligned nanofibrous scaffolds

Electrospun nanofibers are typically collected into a nonwoven membrane, which generally gives random fiber orientation and poor mechanical properties. Most native ECMs found in tissues or organs (e.g. sciatic nerve, heart, tendon, and blood vessel), however, have anisotropic architecture, which is important for tissue function [8]. Therefore, a well-defined architecture is believed to be necessary in order to precisely imitate native ECM for guiding

cell growth or tissue regeneration [51,52]. To this end, electrospun nanofibrous scaffolds with various alignments (e.g. axially aligned, yarn, and radially aligned) have shown superior capacity in shaping cell morphology, guiding cell migration, and affecting cell differentiation when compared to other types of scaffolds both *in vitro* and *in vivo* [48,53,54]. More significantly, specific cellular behaviors (e.g. cell adhesion, migration, and differentiation) of nanofibers may lead to favorable adaptation of cells in this nanoscale microenvironment. A number of strategies have been developed for controlling electrospun nanofiber alignment. Overall, these methods can be classified into three major categories (i.e. mechanical, electrostatic, and magnetic) depending on the type of forces involved [55–58].

Why alignment?

Aligned fibrous scaffolds are advantageous in replicating the ECM for a specific tissue such as cardiac tissue, where the ventricular myocardium is composed of perpendicularly interwoven

collagen strips [59]. An aligned electrospun nanofibrous scaffold can guide the migration and extension of cells [8,60]. For instance, Chew and co-workers showed that aligned electrospun PCL scaffolds were able to provide contact guidance to cultured

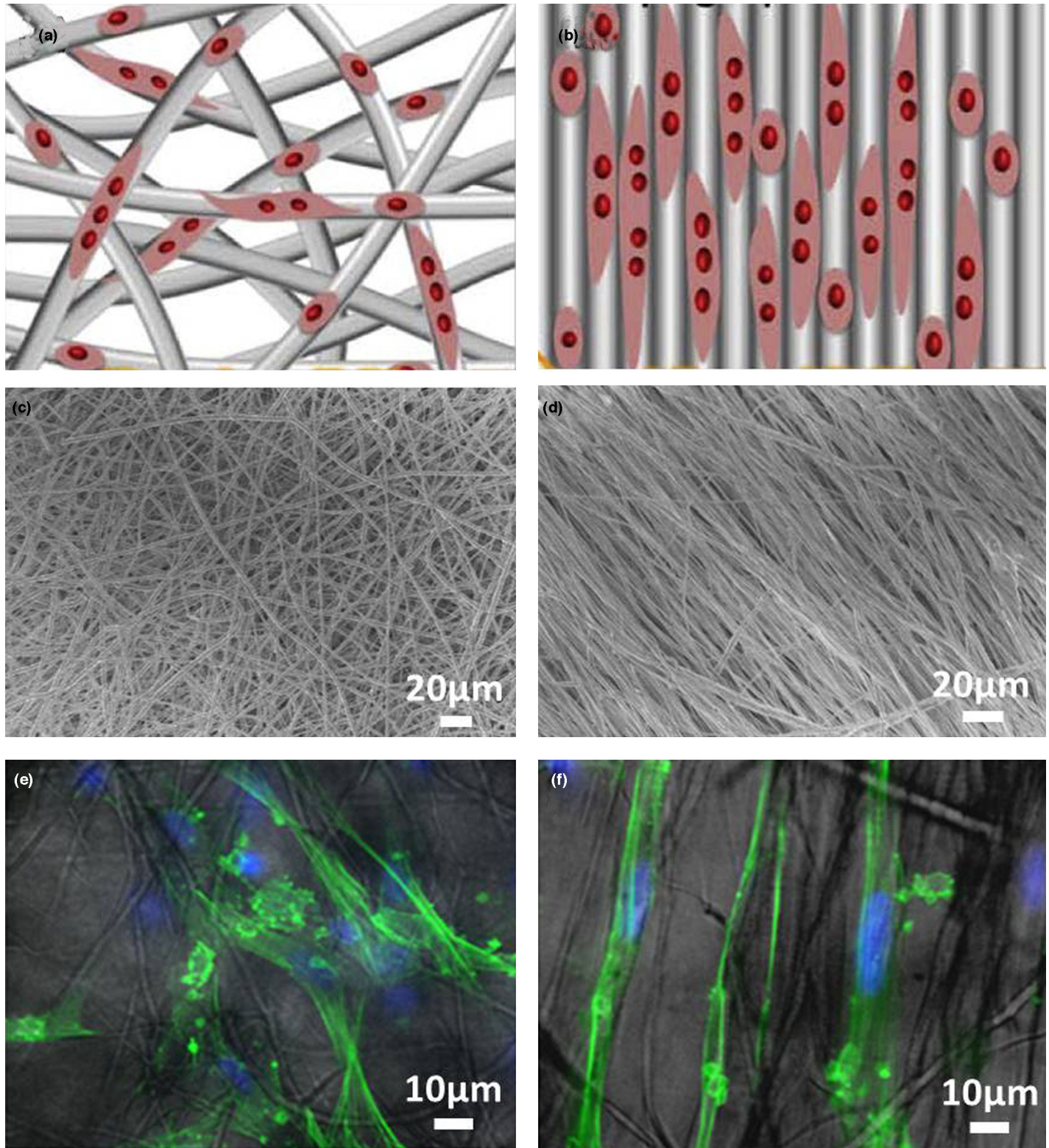


FIGURE 4

Schematic of nanofibers with (a) random orientation and (b) alignment for the guidance of cell migration and extension. Reprinted with permission from [60]. © 2012 Elsevier B.V. (c-f) SEM micrographs of PCL scaffolds for hSC culture: (c) randomly oriented and (d) aligned PCL electrospun fibers; and (e, f) their corresponding fluorescent-light images overlay of hSCs cultured on PCL scaffolds for 3 days. Reprinted with permission from [61]. © 2008 Elsevier B.V.

human Schwann cells (hSCs), resulting in an elongation and alignment of cells along the axes of the fibers [61]. As shown in Fig. 4, the effect of contact guidance provided by the aligned fibers appeared to be more dramatic than the randomly oriented fibers. When cultured on aligned fibers, the cytoskeleton and nuclei align and elongate on the fiber axes. The effect of contact guidance of aligned electrospun fibers on cell morphological changes was also evident in other cell types (e.g. neural stem cell) [62].

Applications of aligned nanofibrous scaffolds in tissue engineering

Significant efforts have been made in the development of aligned nanofibrous structures as tissue-engineered scaffolds for bone [63,64], cartilage [65], dural [53], and other tissues. Natural bone has significant anisotropic mechanical properties with highly oriented ECM and bone cells. Therefore, aligned electrospun nanofibers show great potential as a bone tissue engineering scaffold. Jose

et al. [63] demonstrated that uniaxially aligned PLGA/hydroxyapatite nanofibrous composite membranes could serve as ideal scaffolds for bone tissue engineering and found that the concentration of hydroxyapatite in the composites played an important role in the structure and mechanical behavior of the scaffolds.

Apart from uniaxially aligned nanofibers, some other unique biomimetic aligned fibrous structures have also been developed for tissue engineering applications. Electrospun 3D nanofibrous matrices with high spatial interconnectivity, high porosity, and controlled alignment have been well studied to direct cell orientation and migration (Fig. 5a) [66]. For instance, Cai *et al.* [64] demonstrated a practical 3D macroporous nanofibrous (MNF) scaffold from aligned electrospun nanofibrous yarns for bone tissue engineering (Fig. 5b). Human embryonic stem cell-derived mesenchymal stem cells (hESC-MSCs) were well attached on the 3D MNF scaffolds and the cells changed their original rounded shape to elongated and spindle-like shapes (Fig. 5c). *In vivo*, radiography and histology results showed that the MNF scaffold treated

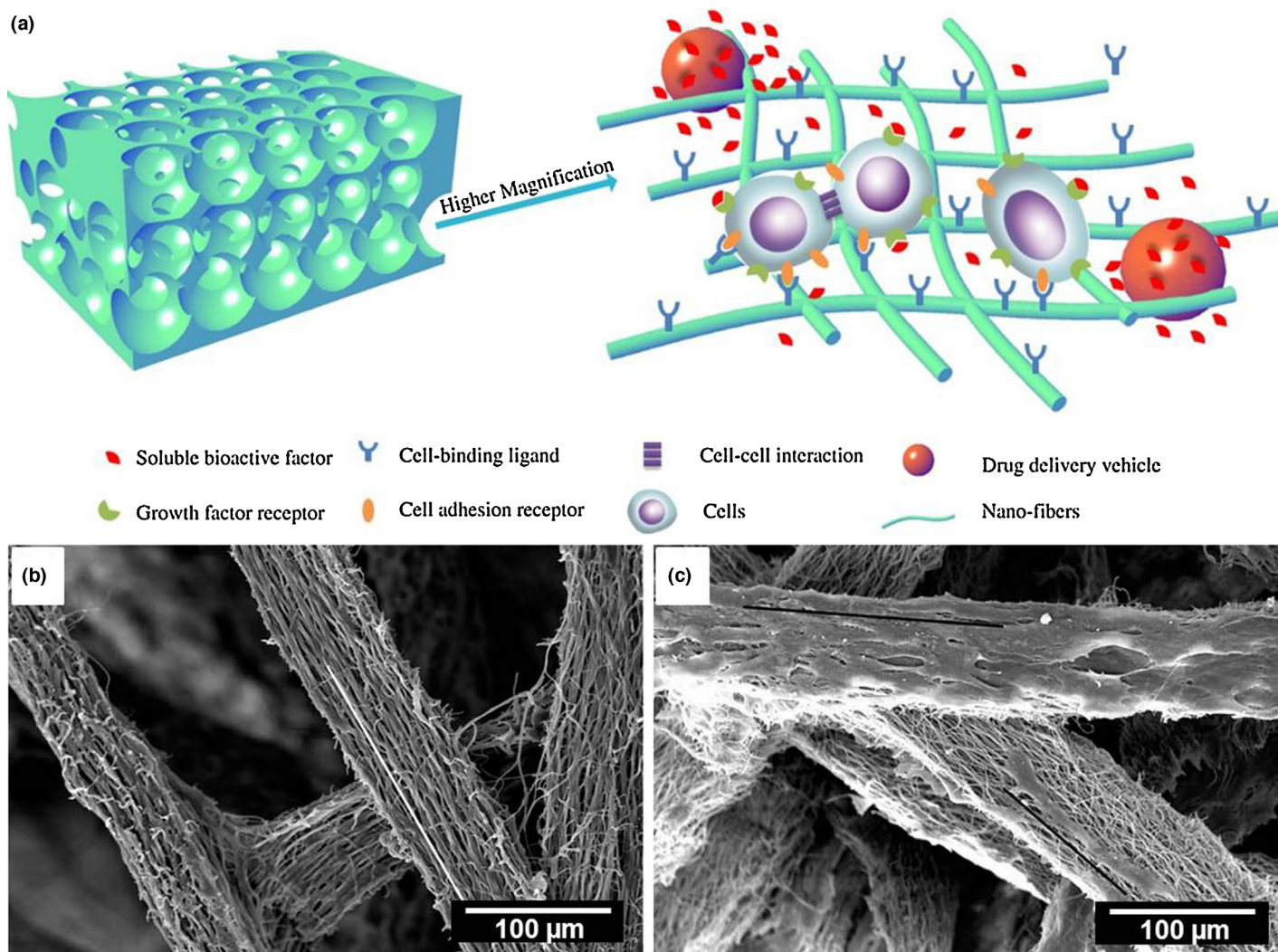


FIGURE 5

(a) Schematic illustration of a biomimetic nanofibrous scaffold with integrated synthetic osteogenic microenvironment. The porous scaffold can not only provide a physical structure that accommodates cells and tissue formation, but also serve as an ECM-mimicking matrix to enhance cell-scaffold interactions and delivery of bioactive agents and/or stem cells in a 3D controlled manner. Reprinted with permission from [66]. © 2012 Elsevier B.V. (b, c) SEM micrographs of 3D MNF scaffolds (b) without and (c) with *in vitro* growth of hESC-MSCs cells (white line indicates the direction of aligned nanofiber, black line indicates the direction of cell elongation). Reprinted with permission from [64]. © 2012 Wiley-VCH Verlag GmbH & Co.

bone defect had fine 3D bony tissue formation around the scaffold as well as inside the scaffold at 6 weeks. This study demonstrated that the 3D MNF scaffold could provide a structural support for hESC-MSC growth and guide bone formation, which may help promote the clinical translation of electrospun nanofibers for regenerative medicine in the future [64].

To imitate the dura mater and to develop artificial dural substitutes to promote cell migration from the surrounding tissue to the center of a dural defect, Xie and co-workers demonstrated the fabrication of an electrospun nanofibrous scaffold consisting of radially aligned PCL nanofibers (Fig. 6) and evaluated its potential application as a dural substitute [53]. This nanofibrous scaffold was

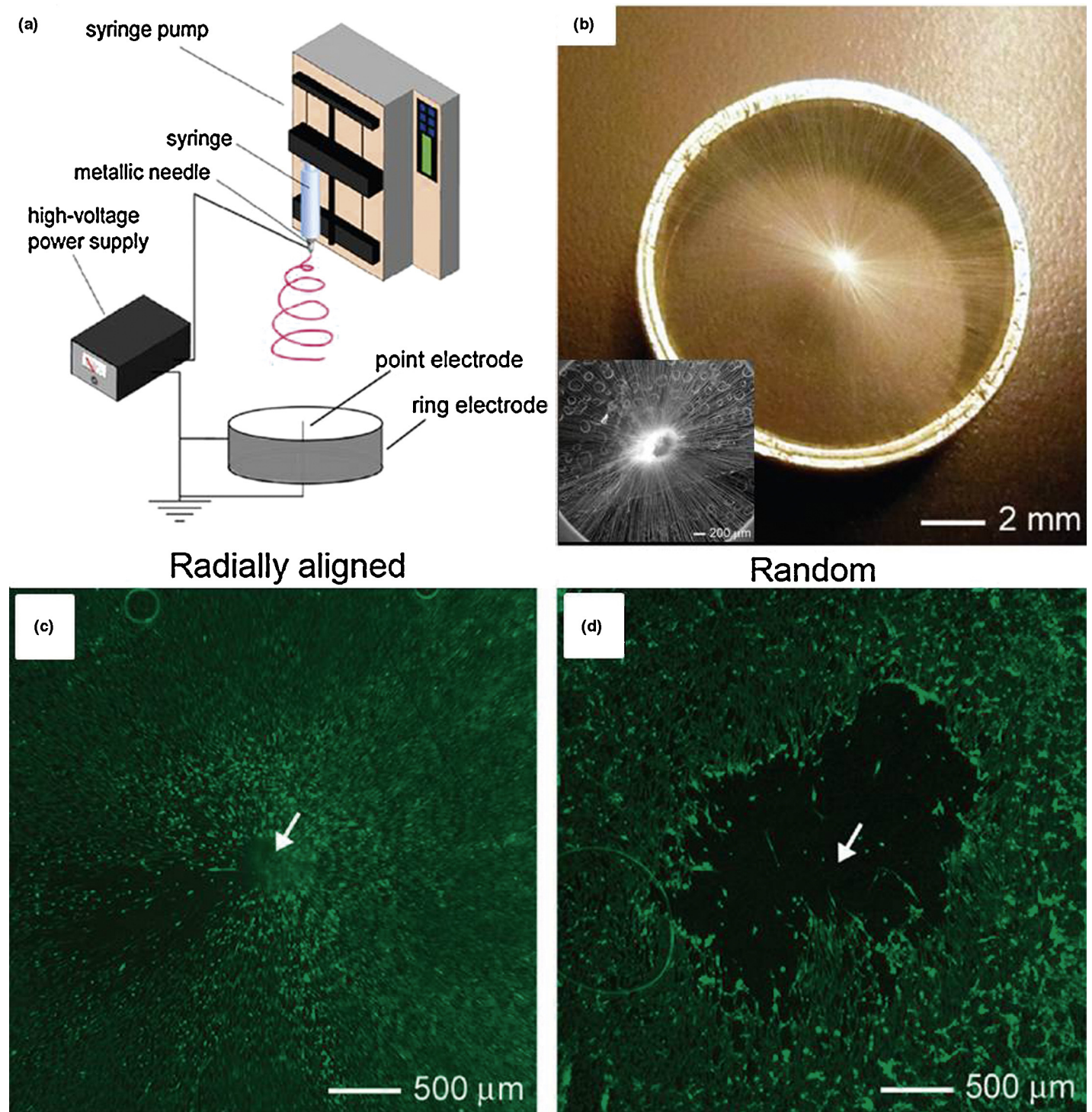


FIGURE 6

(a) Electrospinning setup for generating scaffolds consisting of radially aligned nanofibers. (b) Photograph of a scaffold of radially aligned nanofibers directly deposited on the ring collector. Inset of (b) shows the SEM image of the radial alignment nanofibers. (c, d) Fluorescence micrographs comparing the migration of cells when dura tissues were cultured on scaffolds of random and radially aligned nanofibers, respectively, for 4 days. The dashed circle line indicates the border of dura cells after seeding at day 0. Reprinted with permission from [53]. © 2010 American Chemical Society.

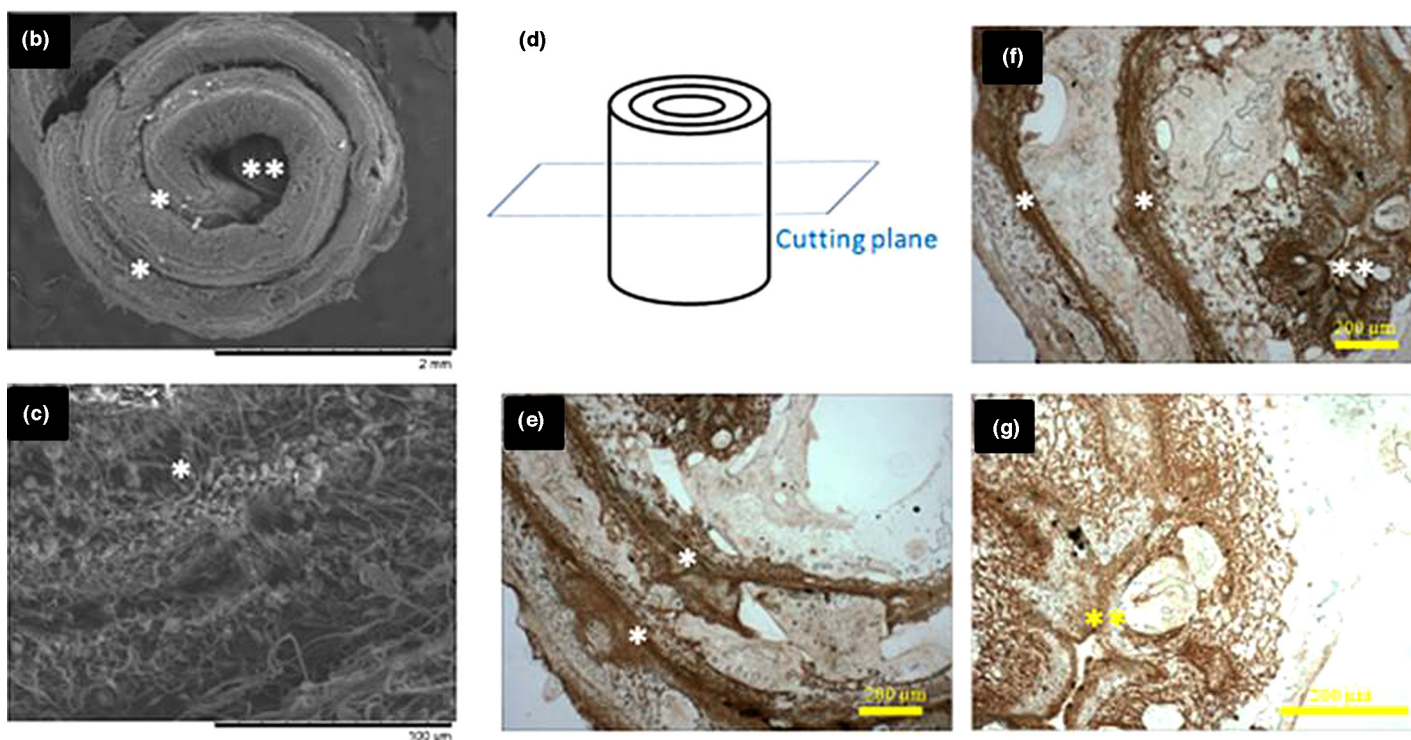
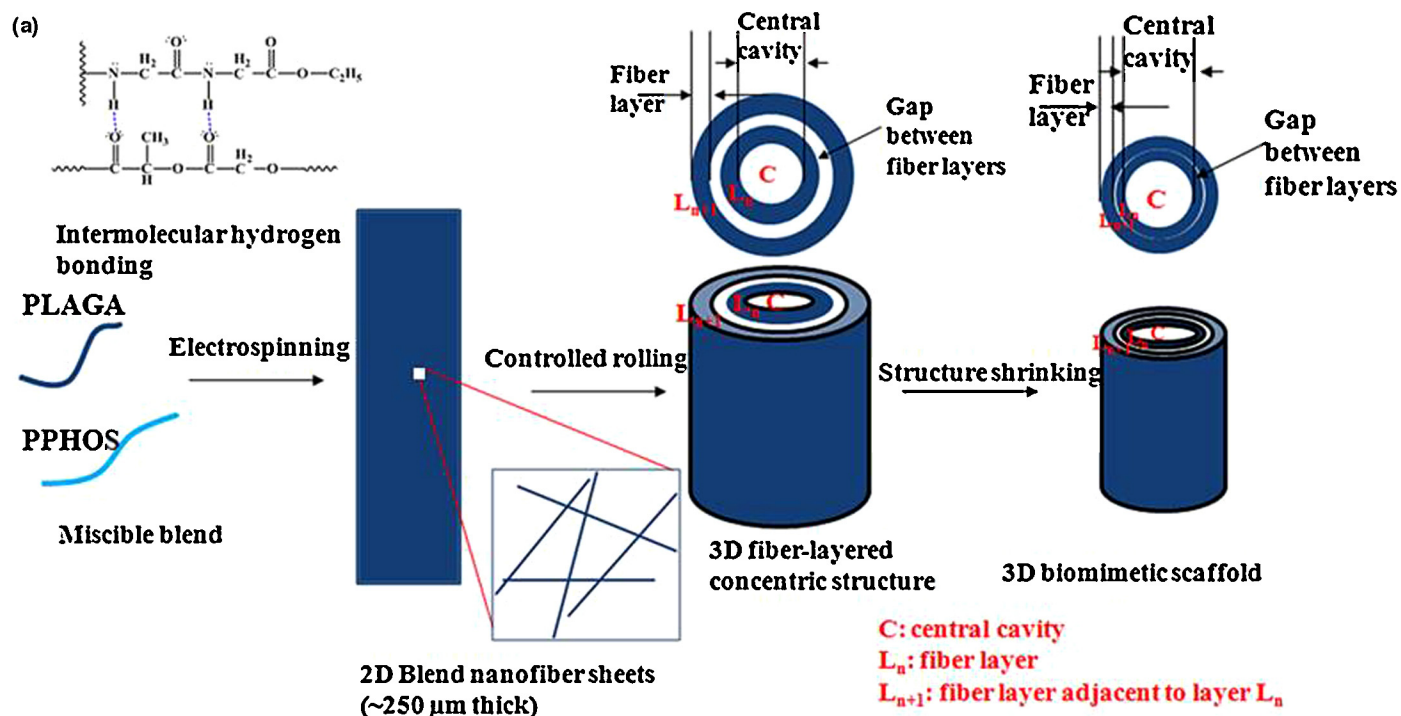


FIGURE 7

(a) Schematics of 3D biomimetic scaffold design and fabrication. ECM deposition throughout 3D scaffold architecture during cell culture. (b, c) SEM images showing the morphologies of cell-seeded 3D biomimetic scaffolds after 28 days of culture: (b) Cell layers covering the scaffold; and (c) ECM deposited by the cells bridging the gaps in the concentric pattern by 28 days. Cells could migrate through 250 μm thick concentric fiber laminates from both the surfaces leading to a homogeneous ECM deposition and cellular activity throughout the biomimetic scaffold. (d–g) Immunohistochemical staining for osteopontin, a prominent component of the mineralized ECM, illustrating a homogenous ECM distribution throughout the scaffold at day 28: (d) Schematics of the select plane for immunohistochemical staining. (e, f) A robust stain for osteopontin bridging the gap between the concentric layers for the lower portion as well as upper and center portion of the 3D biomimetic scaffold. (g) Higher magnification image of the central cavity showing the robust stain for osteopontin. (*) Indicates inter-lamellar space whereas (**) indicates the central cavity. PLAGA: poly(lactide-co-glycolide), PPHOS: poly[(glycine ethyl glycinato)₁(phenylphenoxy)₁phosphazene]. Reprinted with permission from [72]. © 2011 Wiley-VCH Verlag GmbH & Co.

prepared by utilizing a collector composed of a central point electrode and a peripheral ring electrode (Fig. 6a and b). They demonstrated that this novel class of scaffolds was able to present nanoscale topographic cues to cultured cells, directing and enhancing their migration from the periphery to the center. As shown in Fig. 6c, dural fibroblasts stained with fluorescein diacetate (FDA) migrated from the surrounding tissue along the radially aligned nanofibers toward the center of the circular scaffold after incubation for 4 days. In contrast, a void was observed after the same period of incubation time for a scaffold made of random fibers (Fig. 6d), indicating a faster migration rate for the cells on radially aligned nanofibers. Scaffolds based on radially aligned, electrospun nanofibers show great potential as artificial dural substitutes and may be particularly useful as biomedical patches or grafts to induce wound closure and tissue regeneration.

Aligned to random nanofibrous scaffolds

Tendons are the connective tissues that bridge muscle to bone and allow transmission of forces to produce joint movement [67]. They are attached to bones across a specialized transitional tissue with varying structures and compositions. Tendon-related injuries are among the most common injuries to the body. The clinical repair of a tendon-to-bone insertion site often fails due to the lack of regeneration of the complex transitional tissue that normally exists at the uninjured attachment [8,68]. To imitate the gradients in composition and structure that exist at the uninjured tendon-to-bone insertion, Li *et al.* [69] demonstrated the fabrication of a gradient of mineral on the surface of a nanofiber-based scaffold, which could imitate the composition and mechanical function of the tendon-to-bone insertion site. They also demonstrated the fabrication of a nanofibrous scaffold with an “aligned-to-random” transition in the same scaffold by utilization of a specially designed collector, which could imitate the structural organization of collagen fibers at the tendon-to-bone insertion site [67]. Specifically, the aligned portion could imitate the high level of alignment for collagen fibers in a normal tendon and the random portion could recapitulate the less ordered organization of collagen fibers in a bone. Tendon fibroblasts cultured on such an “aligned-to-random” electrospun nanofiber scaffold exhibited highly organized and haphazardly oriented morphologies on the aligned and random portions, respectively. Electrospun nanofiber scaffolds have been demonstrated as a useful platform for repairing injury at a tendon-to-bone insertion site. Future work should focus on investigating the potential of these scaffolds for healing tendon-to-bone insertion in an *in vivo* rotator cuff model.

Spiral-structured nanofibrous scaffolds

Given the pressing clinical need, the market for bone defect reconstruction-based treatments in orthopedics is growing at a rapid rate [70]. Current challenges include the engineering of materials that can match both the mechanical and biological context of real bone tissue matrix and support the vascularization of large tissue constructs [71]. Successful bone regeneration benefits from 3D bioresorbable scaffolds that imitate the hierarchical architecture and mechanical characteristics of native tissue ECM [72,73]. Inspired by the complex hierarchical structures that enable bone functions, Deng and co-workers designed and constructed a 3D biomimetic scaffold by rolling electrospun nanofiber matrices in a concentric

manner with an open central cavity to imitate native bone structurally and mechanically (Fig. 7a) [72]. The fabricated biomimetic scaffolds provide highly desirable properties for bone regeneration. Fig. 7b–g shows ECM deposition throughout 3D scaffold architecture during cell culture. Osteoblast cell layers were formed on the surfaces of biomimetic scaffolds after 28 days of culture (Fig. 7b). Robust osteoblast matrix deposition was found to bridge the gap space between the scaffold’s concentric walls as well as on the nanofiber layers (Fig. 7c), suggesting that the cells were functioning actively. Moreover, the scaffolds exhibited similar lamellar ECM organization to that of native bone. The immunohistochemical staining images shown in Fig. 7e–g demonstrated that robust secretion of osteopontin formed inside the central cavity and the gap space between laminate layers throughout the scaffold.

Another approach for fabricating biomimetic spiral shaped scaffolds involved coating electrospun nanofibers on spiral scaffolds, to provide a substrate that imitates the native ECM and the essential contact guidance cues [10,74]. The spiral structure with open geometries, large surface areas, and porosity is helpful for improving nutrient transport and cell penetration into the scaffolds, which is otherwise limited in conventional tissue-engineered scaffolds for large bone defect repair [10]. Compared with other geometries (e.g. cylindrical and tubular scaffolds), the spiral scaffolds exhibited improved functional performance when dynamic conditions were imitated. Moreover, the spiral walls are thinner than the walls of the tubular and cylindrical scaffolds and are subject to cellular invasion from both sides of the wall, and hence, have a greater ratio of interior to exterior cells than the other scaffolds [74].

Tubular conduit scaffolds

Electrospun nanofibers can be further used to generate scaffolds with complex architectures such as tubular conduits. Tubular



FIGURE 8

Photograph of tubular conduit of 20 cm length and 4 mm inner diameter. Inset is a schematic showing the trilayer tubular conduit (EG/PEG/PG) with spatially designed layers of elastin/gelatine (EG), PDO/elastin/gelatine (PEG), and PDO/gelatine (PG). The lumen layer is rich in protein and outer layers are rich in PDO. Reprinted with permission from [75]. © 2009 Wiley-VCH Verlag GmbH & Co.

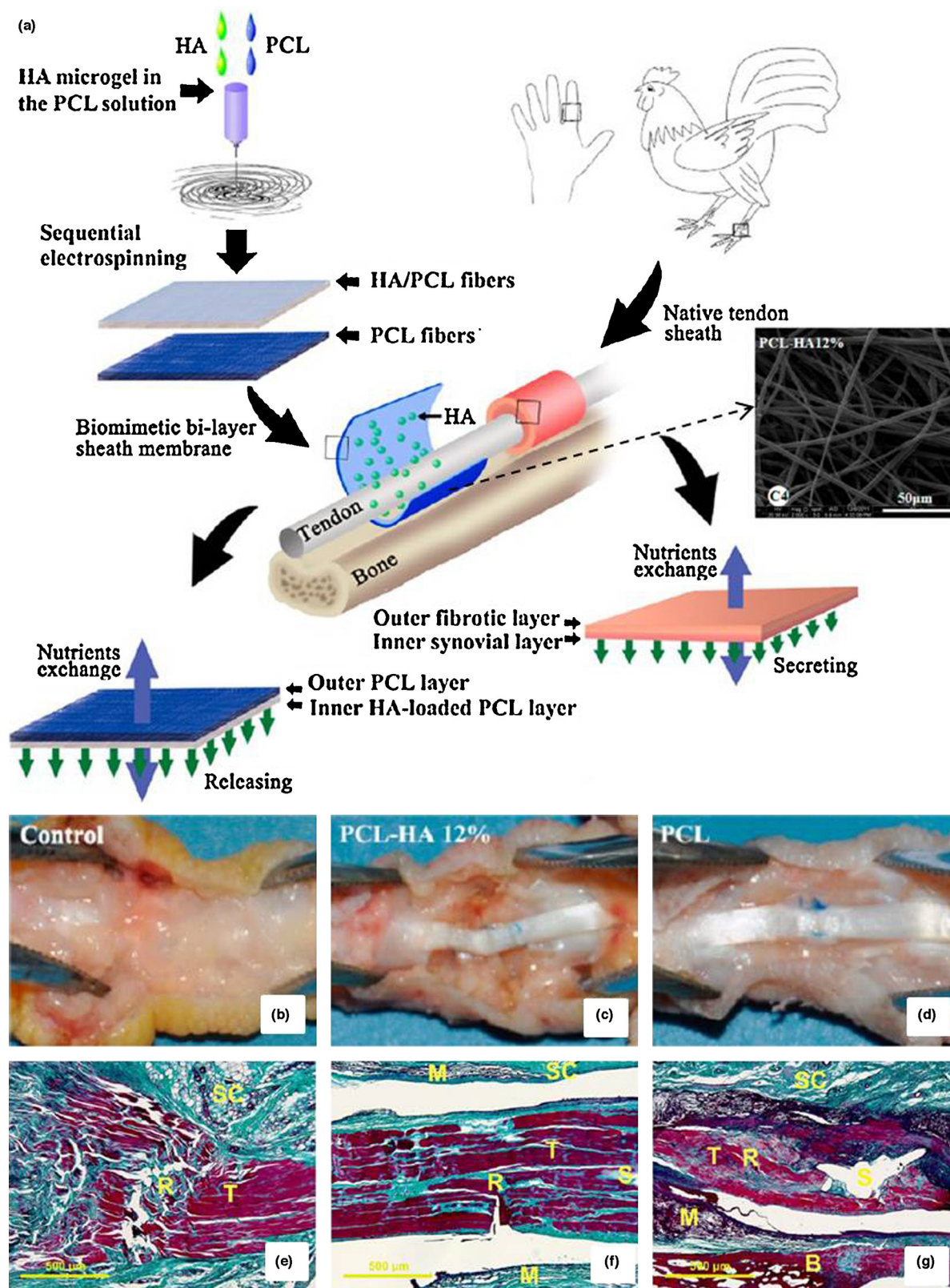


FIGURE 9

(a) After formation of HA microgel in the PCL solution, a biomimetic bilayer sheath membrane was fabricated by sequential electrospinning, producing a sheath membrane consisting of a PCL-HA fibrous membrane as the inner layer and a PCL fibrous membrane as the outer layer to imitate the synovial layer and the fibrotic layer, respectively, of native sheath. (b–d) Gross evaluation of a chicken model of flexor digitorum profundus tendon repair after 21 days. (b) Untreated control group; (c) group treated with sheath membrane with inner PCL-HA PCL layer; (d) group treated with PCL membrane. (e)–(g) Histological assessments of the tendons repaired using each of the treatments. Masson's trichrome staining of untreated repair site (e); repair site wrapped with sheath membrane with inner PCL-HA PCL layer (f); repair site wrapped with PCL membrane (g). Subcutaneous tissue (SC), tendon (T), sutured site (S), bone (B), and materials (M) could be detected. Reprinted with permission from [87]. © 2012 American Chemical Society.

conduits comprised of electrospun fibers can be easily fabricated by collecting nanofibers over a rotating rod of desired diameter (<5 mm) and length (e.g. ~15 cm length for coronary bypass). For example, a trilayer tubular conduit of 20 cm length and 4 mm inner diameter was fabricated by sequential electrospinning of blends of polydioxanone (PDO) and proteins onto a small diameter rod (4 mm), which imitates the complex matrix structure of native arteries (Fig. 8) [75]. Apart from this one-step molding process, a tubular conduit can also be prepared by rolling up electrospun fibrous membranes and securing the edges with solvent, glue, or heating [76]. This strategy allows fabrication of multilayered conduits with aligned fibers in the inner layer and random fibers in the outer layer, which could support better nutrient transport and cell outgrowth without compromising contact guidance [8].

One of the major applications of electrospun nanofibrous tubular conduits is in vascular tissue regeneration. This is because electrospun nanofibrous tubular conduits resemble the hollow structures of vascular or neural tissues. Seamless, nonwoven, bioresorbable vascular prosthetics composed of submicron fibers were fabricated using electrospinning [77], and electrospun collagen and elastin fibers showed promise in vascular tissue engineering [77]. While natural polymer grafts offer excellent cell-matrix interactions, they often lack the mechanical properties of synthetic polymers like PLLA and PGA. When used as a scaffold, these natural polymers rapidly lose strength and dimensional stability, due to gelation and rapid hydrolysis in culture media [75]. Therefore, collagen and elastin-based substances alone are unlikely candidates for vascular tissue engineering, especially under the periodically loaded stress field typical of vascular structures [78]. Similarly, while synthetic polymer grafts offer excellent mechanical properties and easily tailored degradation, they often lack the bioactivity of natural polymers [77]. As such, there has been a great need to create bioresorbable vascular prosthetics that incorporate both the strength of synthetics and the bioactivity of natural polymers. The use of bio-artificial blend nanofibers could be ideal since they not only imitate the dimensions and compositions of ECM, but also have good mechanical properties. Stitzel *et al.* [79] fabricated tubular scaffolds of electrospun PLGA-collagen-elastin ternary blend fibers, and achieved adequate mechanical strength and elasticity and appropriate bioactivities. The electrospinning process allows control of the grafts' mechanical and bioactive properties, which allows for the creation of more dynamic grafts that can closely imitate the behavior and signaling of a native artery [80].

Another application of electrospun nanofibrous tubular conduits is in nerve repair [76]. When direct suturing of two opposing nerve stumps during surgery is not feasible, scaffolds are often used to bridge the damaged nerve gap and to guide nerve regeneration [81]. The scaffold used in nerve tissue engineering applications requires optimal guidance effect, mechanical strength, and cellular compatibility [82]. Electrospun fibrous tubular conduits have shown potential as scaffolds in nerve regeneration applications, as their aligned fibers can provide guidance for axonal growth and the fibrous structure imitates the nerve microenvironment [83]. It has been reported that electrospun fibers could support oriented neurite outgrowth and glial cell migration from dorsal root ganglia explants [84]. *In vivo* studies indicated that nerve conduits with an

inner layer of aligned fibers led to improved peripheral nerve regeneration [85]. *In vitro* investigation showed that, when the filament size was in the subcellular size range, growth cones could easily sense the energy differences of different outgrowth directions. Yao *et al.* [82] developed a fibrous PCL conduit with aligned fibers on the interior surface via electrospinning and determined the optimal fiber diameter in the subcellular size range for neurite extension and directional growth. Neurite length on aligned fibers, with fiber diameters of $3.7 \pm 0.5 \mu\text{m}$ and $5.9 \pm 0.9 \mu\text{m}$, was significantly longer than neurite length on randomly oriented fibers. However, further research should include efforts to design conduits with a suitable degradation profile and optimized fiber organization for better guidance of regenerative axon growth [76].

Biomimetic sheath membrane

The membrane-shaped tendon sheath consists of an outer fibrotic layer and an inner synovial layer. The fibrotic layer prevents exogenous healing of the tendon as an effective biological barrier while the synovial layer secretes synovial fluid (e.g. hyaluronic acid (HA)) to enable tendon gliding [86]. In order to repair damage, biological replication of the tendon sheath is necessary because it allows the tendon to glide smoothly within the sheath. To replicate the hierarchical architecture and complex biologic functions of a native sheath, a biomimetic sheath should consist structurally of an outer antiadhesion layer and an inner lubricant layer. Liu *et al.* [87] fabricated a sheath membrane by sequential electrospinning, producing a biomimetic bilayer sheath membrane consisting of an HA-loaded PCL fibrous membrane as the inner layer and a PCL fibrous membrane as the outer layer, which imitates a native sheath (Fig. 9a). Large and severe peritendinous adhesion areas were found at the repair site in the untreated control group (Fig. 9b and e). In the tendons treated with biomimetic bilayer sheath membrane, no formation of adhesions was observed between the repaired tendons and the peritendinous tissues (Fig. 9c and f). Although the adhesion area could be separated by blunt dissection, loose bundles of fibrous tissue were observed in PCL fibrous membrane treatments (Fig. 9d and g). *In vitro* and *in vivo* results showed that the outer PCL layer could reproduce the antiadhesive role of the outer fibrotic layer while the inner HA loaded PCL layer could imitate the biological function of HA secretion to promote tendon healing and gliding, showing preliminary promise in promoting tendon gliding and preventing adhesion.

Conclusions and outlook

Electrospinning has emerged as an extremely promising method for the preparation of tissue engineering scaffolds. This technique offers advantages for the preparation of scaffolds in terms of resembling the fibrillar structures of ECM, large surface areas, ease of functionalization, and controllable mechanical properties, all of which may lead to improvements in the ability to provide a true biomimetic microenvironment to the developing tissue. Yet important issues regarding its application in tissue engineering, such as achievement of in-depth penetration of cells into scaffolds and control of pore sizes, biomechanical properties, and solvent toxicity still need further investigation [32]. Here, we reviewed the utilization of the electrospinning approach to design and fabricate nanofibrous materials that can be used as biomimetic scaffolds for tissue engineering.

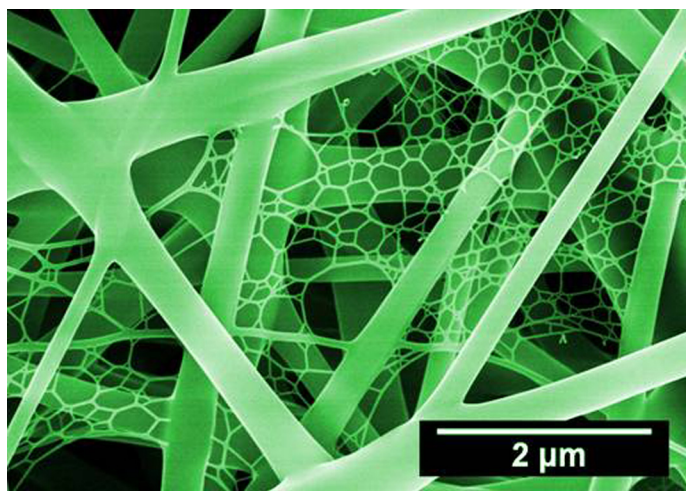


FIGURE 10

SEM image of nano-fiber/net fabricated by ESN technique comprising common electrospun nanofibers and spider-web-like nano-nets. Reprinted with permission from [93]. © 2010 IOP Publishing Ltd.

Despite recent advances toward the development of biomimetic nanofibrous scaffolds for tissue engineering applications, several challenges still remain. Generally, electrospun nanofibers were collected as two-dimensional nonwovens, which limits their applications in 3D tissues. Therefore, one challenge that must be addressed is the complexity of creating 3D porous scaffolds of a clinically relevant 3D shape [88,89]. Fortunately, several attempts have emerged that promise to bridge the gap, for instance, tubular and spiral-structured nanofibrous scaffolds have been fabricated by combining electrospinning with some additive manufacturing technologies, which provide a potential solution to solve this problem. It was recently reported that tissue-mimicking 3D porous scaffolds could be developed by the alternate stacking of cells and thin nanofiber substrate through a layer-by-layer approach [90]. It is expected that the approach can be applied to 3D skin and bone structures [33]. Additionally, it is crucial to develop a strategy capable of producing fibers with a diameter identical to that of native ECM fibers (a diameter less than 100 nm, preferably in the range of 10–50 nm) while maintaining high porosity for cell infiltration and migration [8]. The novel electro-spinning/netting (ESN) technique [91–94] overcomes the bottleneck problem of electrospinning and offers a versatile method for generating spider-web-like nano-nets with ultrafine fiber diameter (less than 50 nm) while maintaining high porosity (Fig. 10), which make nano-nets optimal candidates for the fabrication of tissue-engineering scaffolds.

Although many challenges remain, electrospinning exhibited great potential in the fabrication of fibrous scaffolds with controllable compositions and structures, enabling scientists from various disciplines to design and generate novel scaffolds incorporating various biomimetic characteristics at genetic, molecular, and nanometer scales [3]. We envision a continuous expansion of the electrospinning approach in biomimetic scaffold design in the coming decades, which will stimulate further research and advances in the exciting field of tissue engineering.

Acknowledgements

We acknowledge financial support from the West Virginia Higher Education Policy Commission/Division of Science Research, NSF,

and AO Foundation (Project S-13-15L was supported by the AO Foundation). We thank Suzanne Danley for proofreading.

References

- 1 T. Dvir, et al. *Nat. Nanotechnol.* 6 (2011) 13.
- 2 M.M. Stevens, J.H. George, *Science* 310 (2005) 1135.
- 3 P.X. Ma, *Adv. Drug Deliv. Rev.* 60 (2008) 184.
- 4 Y.P. Li, et al. *Angew. Chem. Int. Ed.* 51 (2012) 2864.
- 5 X.H. Zhang, et al. *Adv. Drug Deliv. Rev.* 61 (2009) 988.
- 6 J. Du, et al. *Biomaterials* 32 (2011) 5427.
- 7 J.A. Du, K.J. Yarema, *Adv. Drug Deliv. Rev.* 62 (2010) 671.
- 8 W. Liu, et al. *Adv. Health. Mater.* 1 (2012) 10.
- 9 J.M. Holzwarth, P.X. Ma, *Biomaterials* 32 (2011) 9622.
- 10 J.P. Wang, et al. *J. Biomed. Mater. Res. Part A* 93A (2010) 753.
- 11 S. Liao, et al. *Biomed. Mater.* 1 (2006) R45.
- 12 B.B. Jiang, et al. *Biomacromolecules* 11 (2010) 3630.
- 13 L.G. Griffith, G. Naughton, *Science* 295 (2002) 1009.
- 14 M. Goldberg, et al. *J. Biomater. Sci. Polym. Ed.* 18 (2007) 241.
- 15 Y.P. Li, et al. *ACS Nano* 6 (2012) 9485.
- 16 R. Vasita, D.S. Katti, *Int. J. Nanomed.* 1 (2006) 15.
- 17 P.X. Ma, R.Y. Zhang, *J. Biomed. Mater. Res.* 46 (1999) 60.
- 18 T.C. Holmes, et al. *Proc. Natl. Acad. Sci. U. S. A.* 97 (2000) 6728.
- 19 X.H. Liu, et al. *Nat. Mater.* 10 (2011) 398.
- 20 R.J. Wade, J.A. Burdick, *Mater. Today* 15 (2012) 454.
- 21 J.B. Matson, et al. *Curr. Opin. Solid State Mater. Sci.* 15 (2011) 225.
- 22 J.D. Hartgerink, et al. *Proc. Natl. Acad. Sci. U. S. A.* 99 (2002) 5133.
- 23 W.J. Li, et al. *J. Biomed. Mater. Res.* 60 (2002) 613.
- 24 N. Bhardwaj, S.C. Kundu, *Biotechnol. Adv.* 28 (2010) 325.
- 25 S.R. Bhattarai, et al. *Biomaterials* 25 (2004) 2595.
- 26 J. Shi, et al. *ACS Appl. Mater. Interfaces* 2 (2010) 1025.
- 27 H.R. Pant, et al. *Colloid Surf. B: Biointerfaces* 88 (2011) 587.
- 28 S. Ramakrishna, et al. *Mater. Today* 9 (2006) 40.
- 29 J. Liu, et al. *Small* 5 (2009) 536.
- 30 H. Fong, et al. *Polymer* 40 (1999) 4585.
- 31 D. Li, Y.N. Xia, *Adv. Mater.* 16 (2004) 1151.
- 32 S. Agarwal, et al. *Adv. Mater.* 21 (2009) 3343.
- 33 J.H. Jang, et al. *Adv. Drug Deliv. Rev.* 61 (2009) 1065.
- 34 Z.M. Huang, et al. *Compos. Sci. Technol.* 63 (2003) 2223.
- 35 M.M. Hohman, et al. *Phys. Fluids* 13 (2001) 2201.
- 36 A.L. Yarin, et al. *J. Appl. Phys.* 89 (2001) 3018.
- 37 M. Bognitzki, et al. *Adv. Mater.* 13 (2001) 70.
- 38 A. Greiner, J.H. Wendorff, *Angew. Chem. Int. Ed.* 46 (2007) 5670.
- 39 B.D. Ulery, et al. *J. Polym. Sci. Pt. B: Polym. Phys.* 49 (2011) 832.
- 40 B. Ding, et al. *Mater. Today* 13 (2010) 16.
- 41 X.F. Wang, et al. *Nano Today* 6 (2011) 510.
- 42 P. Roach, et al. *Soft Matter* 4 (2008) 224.
- 43 R. Chen, J.A. Hunt, *J. Mater. Chem.* 17 (2007) 3974.
- 44 J.Y. Lin, et al. *Crit. Rev. Solid State Mater. Sci.* 37 (2012) 94.
- 45 V.J. Reddy, et al. *Wound Repair Regen.* 21 (2013) 1.
- 46 J. Wang, X. Yu, *Acta Biomater.* 6 (2010) 3004.
- 47 T.B.L. Nguyen, B.T. Lee, *J. Biomater. Appl.* 27 (2012) 255.
- 48 C.Y. Huang, et al. *Biomaterials* 33 (2012) 1791.
- 49 M.M. Stevens, *Mater. Today* 11 (2008) 18.
- 50 M. Deng, et al. *IEEE Trans. Nanobiosci.* 11 (2012) 3.
- 51 T.G. Kim, et al. *Adv. Funct. Mater.* 22 (2012) 2446.
- 52 F. Yang, et al. *Biomaterials* 26 (2005) 2603.
- 53 J. Xie, et al. *ACS Nano* 4 (2010) 5027.
- 54 L.S. Wan, Z.K. Xu, *J. Biomed. Mater. Res. A* 89 (2009) 168.
- 55 D. Li, et al. *Adv. Mater.* 16 (2004) 361.
- 56 D. Yang, et al. *Adv. Mater.* 19 (2007) 3702.
- 57 J.A. Matthews, et al. *Biomacromolecules* 3 (2002) 232.
- 58 W.E. Teo, S. Ramakrishna, *Nanotechnology* 17 (2006) R89.
- 59 G.C. Engelmayr, et al. *Nat. Mater.* 7 (2008) 1003.
- 60 M. Chen, et al. *Acta Biomater.* 9 (2013) 5562.
- 61 S.Y. Chew, et al. *Biomaterials* 29 (2008) 653.
- 62 L. He, et al. *Acta Biomater.* 6 (2010) 2960.
- 63 M.V. Jose, et al. *Acta Biomater.* 5 (2009) 305.
- 64 Y.Z. Cai, et al. *J. Biomed. Mater. Res. A* 100 (2012) 1187.
- 65 J.P. Chen, C.H. Su, *Acta Biomater.* 7 (2011) 234.
- 66 Z.P. Zhang, et al. *Adv. Drug Deliv. Rev.* 64 (2012) 1129.
- 67 J.W. Xie, et al. *Nanoscale* 2 (2010) 923.
- 68 L.E. Richardson, et al. *Trends Biotechnol.* 25 (2007) 409.

- 69 X.R. Li, et al. *Nano Lett.* 9 (2009) 2763.
70 B.B. Jiang, B.Y. Li, *J. Biomed. Mater. Res. B* 88B (2009) 332.
71 B.Y. Li, et al. *Biomaterials* 30 (2009) 2552.
72 M. Deng, et al. *Adv. Funct. Mater.* 21 (2011) 2641.
73 J.H. Lee, et al. *Biomaterials* 33 (2012) 999.
74 C.M. Valmikinathan, et al. *Mater. Sci. Eng. C: Mater. Biol. Appl.* 31 (2011) 22.
75 V. Thomas, et al. *Biotechnol. Bioeng.* 104 (2009) 1025.
76 J.W. Xie, et al. *Nanoscale* 2 (2010) 35.
77 S.A. Sell, G.L. Bowlin, *J. Mater. Chem.* 18 (2008) 260.
78 S.J. Lee, et al. *J. Biomed. Mater. Res. A* 83A (2007) 999.
79 J. Stitzel, et al. *Biomaterials* 27 (2006) 1088.
80 S. Agarwal, et al. *Polymer* 49 (2008) 5603.
81 C.A. Bashur, et al. *Biomaterials* 27 (2006) 5681.
82 L. Yao, et al. *J. Biomed. Mater. Res. B* 90B (2009) 483.
83 L.M.Y. Yu, et al. *Mater. Today* 11 (2008) 36.
84 E. Schnell, et al. *Biomaterials* 28 (2007) 3012.
85 S.Y. Chew, et al. *Adv. Funct. Mater.* 17 (2007) 1288.
86 P. Sharma, N. Maffulli, *J. Bone Joint Surg. Am.* 87A (2005) 187.
87 S. Liu, et al. *Biomacromolecules* 13 (2012) 3611.
88 J.M. Holzwarth, P.X. Ma, *J. Mater. Chem.* 21 (2011) 10243.
89 H.J. Wang, C.A. van Blitterswijk, *Biomaterials* 31 (2010) 4322.
90 X.C. Yang, et al. *Tissue Eng. A* 15 (2009) 945.
91 X.F. Wang, et al. *Nanoscale* 3 (2011) 911.
92 B. Ding, et al. *J. Mater. Chem.* 21 (2011) 12784.
93 X.F. Wang, et al. *Nanotechnology* 21 (2010) 055502.
94 N.A.M. Barakat, et al. *Polymer* 50 (2009) 4389.
95 X. Zhang, et al. *J. Mater. Chem.* 18 (2008) 621.
96 W. Barthlott, C. Neinhuis, *Planta* 202 (1997) 1.
97 L. Jiang, et al. *Angew. Chem. Int. Ed.* 43 (2004) 4338.
98 Y. Miyauchi, et al. *Nanotechnology* 17 (2006) 5151.
99 Z.G. Guo, W.M. Liu, *Plant Sci.* 172 (2007) 1103.
100 L. Feng, et al. *Adv. Mater.* 14 (2002) 1857.
101 D. Li, et al. *Nano Lett.* 3 (2003) 1167.
102 G.D. Yan, et al. *Langmuir* 27 (2011) 4285.
103 R.E. Grojean, et al. *Appl. Optics* 19 (1980) 339.
104 Y. Zhao, et al. *J. Am. Chem. Soc.* 129 (2007) 764.